Fast shuttling of a trapped ion in the presence of noise

Xiao-Jing Lu,[1,2] J. G. Muga,[1,2] Xi Chen,[1] U. G. Poschinger,[3] F. Schmidt-Kaler,[3] and A. Ruschhaupt[4]
[1]*Department of Physics, Shanghai University, 200444 Shanghai, People's Republic of China*
[2]*Departamento de Química Física, UPV/EHU, Apdo. 644, E-48080 Bilbao, Spain*
[3]*QUANTUM, Institut für Physik, Universität Mainz, D-55128 Mainz, Germany*
[4]*Department of Physics, University College Cork, Cork, Ireland*
(Received 16 April 2014; published 18 June 2014)

We theoretically investigate the motional excitation of a single ion caused by spring-constant and position fluctuations of a harmonic trap during trap shuttling processes. A detailed study of the sensitivity on noise for several transport protocols and noise spectra is provided. The effect of slow spring-constant drifts is also analyzed. Trap trajectories that minimize the excitation are designed combining invariant-based inverse engineering, perturbation theory, and optimal control.

DOI: 10.1103/PhysRevA.89.063414 PACS number(s): 37.10.Ty, 03.67.Lx

I. INTRODUCTION

A quantum information processing architecture based on shuttling individual or small groups of ions among different storing or processing sites requires fast transporting techniques that avoid decoherence and excitations at the arrival zone [1–3]. A promising research and technological avenue [4,5] has been opened by recent experiments [2,6,7] that demonstrate the feasibility of a transport-based architecture, even beyond (faster than) the adiabatic regime [8,9]. Such experiments on transport and fast splitting of ion crystals have been performed with optimized time-dependent control voltages and the outcome is analyzed with spectroscopy precise at the level of single motional quanta [8,9]. One major limitation is given by the fact that only finite voltages can be switched in finite time. However, if smaller traps are employed, smaller voltages are needed. Then, noise levels increase due to closer proximity to surfaces. Thus, one can consider the presence of noise to be the ultimate limitation, as both the attainable trap sizes and the switchable voltages are technical limitations. Electric field noise in Paul traps has been characterized experimentally in Ref. [10] by monitoring the heating out of the motional ground state. It was found that the corresponding noise level exceeds the limit given by Johnson noise by several orders of magnitude, an effect that has been termed *anomalous heating*. In a resting trap, it has been shown [11] that the heating rate is determined by the noise power spectral density at the trap frequency. This does not necessarily hold for shuttling operations, where a broader part of the noise spectrum and slow drifts of the trap parameters can compromise the shuttling result producing undesired excitation.

On many ion trap experiments, the frequency dependence of the electric field noise spectral density $S(\Omega)$ has been investigated by measuring heating rates for varying trap frequencies, and commonly a polynomial scaling $S(\Omega) \propto \Omega^{-\mu}$ is observed. While a wide range of exponents μ between -1 and 6 have been reported [12], in many cases a behavior consistent with flicker noise $\mu \approx 1$ is observed. This indicates that a variety of noise spectra can occur and that resonances of technical origin can play a role. Fast shuttling operations ultimately require rapidly changing voltage wave forms [13,14], which strongly restricts the possibility of mitigating noise by filtering. This leads us to the conclusion that it is worthwhile to investigate the sensitivity of shuttling protocols for colored noise, and their optimization. We also consider drifts of trap parameters, which are slow on the time scales of the trap period and the durations of shuttling operations. These drifts can be characterized by monitoring the trap frequency over time. On a trap similar to the design used in [9], we find long-time variations of the trap frequency of up to 5%. These variations can be caused by drift of the trap voltages, thermal expansion of the trap, and charging of the trap itself.

In Sec. II we review how faster than adiabatic trap trajectories without final excitation (*shortcut to adiabaticity*) may be designed using invariant-based inverse engineering [15–19]. In Sec. III, we shall consider two basic types of noise that affect a moving harmonic trap: spring-constant fluctuations and position fluctuations around the ideal trajectory (trap shaking). We provide general results for the final excitation energy for different noise power spectra by using a perturbative master-equation approach.

In Sec. IV, trajectories are found that minimize the effect of a systematic (constant, not random) spring constant error. Finally, we discuss how our theoretical results may be implemented experimentally.

II. INVARIANT-BASED INVERSE ENGINEERING METHOD

The invariant-based inverse engineering method has been successfully applied to various quantum control problems. While it has been used to design protocols for fast ion shuttling [15–19], it has also been employed in the field of internal-state control to find protocols which are resilient to noise [20,21]. In this section, we provide a brief review of this method for the ion-shuttling scenario.

The harmonic transport of one ion is described here by the effective 1D Hamiltonian,

$$\hat{H}_0(t) = \frac{\hat{p}^2}{2m} + \frac{1}{2}m\omega^2[\hat{q} - x(t)]^2, \tag{1}$$

where $\hat{q}$ and $\hat{p}$ are the position and momentum operators, $\omega/(2\pi)$ is the frequency of the trap, and $x(t)$ its center. The corresponding quadratic-in-momentum Lewis-Riesenfeld invariant [22–24] is given in this case (up to an arbitrary

multiplicative constant) by [15]

$$\hat{I}(t) = \frac{1}{2m}(\hat{p} - m\dot{x}_c)^2 + \frac{1}{2}m\omega^2[\hat{q} - x_c(t)]^2, \tag{2}$$

where the function $x_c(t)$ must satisfy the auxiliary equation,

$$\ddot{x}_c + \omega^2(x_c - x) = 0, \tag{3}$$

to guarantee the invariant condition,

$$\frac{d\hat{I}(t)}{dt} \equiv \frac{\partial \hat{I}(t)}{\partial t} + \frac{1}{i\hbar}[\hat{I}(t), \hat{H}_0(t)] = 0. \tag{4}$$

The expectation value of $\hat{I}(t)$ remains constant for solutions of the time-dependent Schrödinger equation $i\hbar\partial_t\Psi(q,t) = \hat{H}_0(t)\Psi(q,t)$. They can be expressed in terms of independent "transport modes" $\Phi(q,t;n) = e^{i\theta(n)}\phi(q,t;n)$ as $\Psi(q,t) = \sum_n c(n)\Phi(q,t;n)$, where $n = 0,1,...$ (n will be used hereafter to denote the mode); $c(n)$ are time-independent coefficients; and $\phi(q,t;n)$ are the orthonormal eigenvectors of the invariant $\hat{I}(t)$ satisfying $\hat{I}(t)\phi(q,t;n) = \lambda(n)\phi(q,t;n)$, with real time-independent $\lambda(n)$. The Lewis-Riesenfeld phase is

$$\theta(t;n) = \frac{1}{\hbar}\int_0^t \langle\phi(t';n)|i\hbar\frac{\partial}{\partial t'} - \hat{H}_0(t')|\phi(t';n)\rangle dt'. \tag{5}$$

For the harmonic trap considered here [15],

$$\phi(q,t;n) = \exp\left(i\frac{m\dot{x}_c q}{\hbar}\right)\phi^{(0)}(q - x_c;n), \tag{6}$$

where $\phi^{(0)}(q;n)$ are the eigenstates of Eq. (1) for $x(t) = 0$. Note that x_c is the center of mass of the transport modes obeying the classical Newton equation (3).

Suppose that the harmonic trap is displaced from $x(0) = 0$ to $x(T) = d$ in a shuttling time T. The trajectory $x(t)$ of the trap can be inverse engineered by designing first an appropriate classical trajectory $x_c(t)$. To guarantee the commutativity of $\hat{I}(t)$ and $\hat{H}_0(t)$ at $t = 0$ and $t = T$, which implies the mapping between initial and final trap eigenstates without final excitation, we set the conditions [15]:

$$\begin{aligned} x(0) = x_c(0) = 0, \quad \dot{x}_c(0) = 0, \\ x(T) = x_c(T) = d, \quad \dot{x}_c(T) = 0. \end{aligned} \tag{7}$$

The additional conditions,

$$\ddot{x}_c(0) = 0, \quad \ddot{x}_c(T) = 0, \tag{8}$$

may be imposed to avoid sudden jumps in the trap position. However, discontinuities of $\ddot{x}_c(t)$ may in general be allowed: They correspond to ideal instantaneous trap displacements inducing a sudden finite jump of the acceleration, whereas the velocity $\dot{x}_c(t)$ and the trajectory $x_c(t)$ remain continuous. In the following, we consider for simplicity the transport of the single mode n in the noiseless limit ($n = 0$ in the numerical examples), and examine the excitation energy of the system energy due to noise or errors, as well as ways to suppress or minimize it.

III. NOISE

To study the effect of the noise we follow the master equation treatment in [25–27]. The Hamiltonian is assumed to be of the form,

$$\hat{H}(t) = \frac{\hat{p}^2}{2m} + \frac{1}{2}m\omega^2[\hat{q} - x(t)]^2 + \xi(t)\hat{L}, \tag{9}$$

where ω is constant, $\hat{L}$ is a system operator coupling to the environment, and $\xi(t)$ is a fluctuating variable that satisfies

$$\mathcal{E}[\xi(t)] = 0, \ \mathcal{E}[\xi(t)\xi(t')] = \alpha(t - t'), \tag{10}$$

where $\alpha(t - t')$ is the correlation function of the noise and $\mathcal{E}[...]$ the statistical expectation. The correlation function and the spectral power density are related by the Wiener-Khinchin theorem,

$$S(\Omega) = \frac{1}{2\pi}\int_{-\infty}^{\infty}\alpha(\tau)\cos(\Omega\tau)d\tau, \tag{11}$$

$$\alpha(\tau) = \int_{-\infty}^{\infty}S(\Omega)\cos(\Omega\tau)d\Omega. \tag{12}$$

By expanding in the ratio between environmental correlation time and the typical time scale of the system [28], a closed master equation can be derived retaining first-order corrections to the Markovian limit,

$$\frac{d}{dt}\hat{\rho} = -\frac{i}{\hbar}[\hat{H}_0, \hat{\rho}] + \frac{1}{\hbar}[\hat{L}, \hat{\rho}\hat{O}(t)^\dagger] - \frac{1}{\hbar}[\hat{L}^\dagger, \hat{O}(t)\hat{\rho}], \tag{13}$$

where

$$\hat{O}(t) = \frac{1}{\hbar}g(t)\hat{L} - \frac{i}{\hbar^2}f(t)[\hat{H}_0, \hat{L}] - \frac{h(t)}{\hbar^3}[\hat{L}^\dagger, \hat{L}]\hat{L}, \tag{14}$$

and

$$g(t) = \int_0^t \alpha(t - t')dt', \tag{15}$$

$$f(t) = \int_0^t \alpha(t - t')(t - t')dt', \tag{16}$$

$$h(t) = \int_0^t\int_0^{t'} \alpha(t - t')\alpha(t' - u)(t - t')du\,dt'. \tag{17}$$

We insist that the master equation (13) is valid on the condition that the noise correlation time is small compared to the typical system time scales, so that f and h terms must be corrections to the dominant g term.

A. Spring constant noise

We consider now a fluctuating spring constant $\omega^2(1 + \xi(t))$, where ω is fixed and $\xi(t)$ is a fluctuating function that satisfies Eq. (10). According to Eqs. (9) and (10) we set $\hat{L} = \frac{1}{2}m\omega^2(\hat{q} - x)^2$ so that

$$\hat{H}(t) = \frac{\hat{p}^2}{2m} + \frac{1}{2}m\omega^2[1 + \xi(t)][\hat{q} - x(t)]^2, \tag{18}$$

$$\hat{O}(t) = \frac{m\omega^2}{2\hbar}g(t)(\hat{q} - x)^2 + \frac{2}{m\hbar}f(t)\left[\hat{p}x - \frac{1}{2}(\hat{p}\hat{q} + \hat{q}\hat{p})\right], \tag{19}$$

and the master equation (13) becomes

$$\frac{d}{dt}\hat{\rho} = -\frac{i}{\hbar}[\hat{H}_0,\hat{\rho}] - \frac{m^2\omega^4}{4\hbar^2}g(t)[(\hat{q}-x)^2,\ [(\hat{q}-x)^2,\hat{\rho}]] - \frac{m\omega^4}{2\hbar^2}f(t)\left[(\hat{q}-x)^2,\ [\hat{p}x - \frac{1}{2}(\hat{p}\hat{q}+\hat{q}\hat{p}),\hat{\rho}]\right]. \tag{20}$$

Using time-dependent perturbation theory for the master equation we may write the density operator as (for an alternative nonperturbative approach see Appendix A)

$$\hat{\rho}(T) \simeq \hat{\rho}_0(T) + \frac{m^2\omega^4}{4\hbar^2}\int_0^T g(t)\widetilde{U}_0(T,t)\widetilde{J}_1(t)\hat{\rho}_0(t)dt + \frac{m\omega^4}{2\hbar^2}\int_0^T f(t)\widetilde{U}_0(T,t)\widetilde{J}_2(t)\hat{\rho}_0(t)dt, \tag{21}$$

where $\hat{\rho}_0(T) = |\Phi(T;n)\rangle\langle\Phi(T;n)|$ is the state for noiseless unitary dynamics in the transport mode n, and $\widetilde{U}_0(T,t)$ is the noiseless evolution superoperator, i.e.,

$$\hat{\rho}_0(t) = \widetilde{U}_0(t,t')\hat{\rho}_0(t') = \hat{U}_0(t,t')\hat{\rho}_0(t')\hat{U}_0^\dagger(t,t'); \tag{22}$$

$\hat{U}_0(t,t')$ is the noiseless evolution operator, and $\widetilde{J}_1(t)$ and $\widetilde{J}_2(t)$ are superoperators,

$$\widetilde{J}_1(t)\hat{\rho}_0(t) = -[(\hat{q}-x)^2,[(\hat{q}-x)^2,\hat{\rho}_0(t)]], \tag{23}$$

$$\widetilde{J}_2(t)\hat{\rho}_0(t) = -\left[(\hat{q}-x)^2,\left[\hat{p}x - \frac{(\hat{p}\hat{q}+\hat{q}\hat{p})}{2},\hat{\rho}_0(t)\right]\right]. \tag{24}$$

A detailed calculation gives the final energy corresponding to an initial state in the $n_{\rm th}$ mode,

$$\begin{aligned}\langle\hat{H}(T)\rangle &= \mathrm{tr}[\hat{H}_0(T)\hat{\rho}(T)] \simeq \langle\Phi(T;n)|\hat{H}_0(T)|\Phi(T;n)\rangle \\ &+\frac{m^2\omega^4}{4\hbar^2}\int_0^T g(t)\langle\Phi(t;n)|\widetilde{J}_1(t)\hat{H}'(t)|\Phi(t;n)\rangle dt \\ &+\frac{m\omega^4}{2\hbar^2}\int_0^T f(t)\langle\Phi(t;n)|\widetilde{J}_3(t)\hat{H}'(t)|\Phi(t;n)\rangle dt \\ &= E(n) + \hbar\omega^3\left(n+\frac{1}{2}\right)\int_0^T g(t)dt, \\ &+m\int_0^T [g(t)\ddot{x}_c^2(t) + \omega^2 f(t)\dot{x}_c(t)\ddot{x}_c(t)]dt,\end{aligned} \tag{25}$$

where $E(n) = (n+1/2)\hbar\omega$,

$$\widetilde{J}_3(t)\hat{H}'(t) = -\left[\hat{p}x - \frac{1}{2}(\hat{p}\hat{q}+\hat{q}\hat{p}),[(\hat{q}-x)^2,\hat{H}'(t)]\right],$$

and $\hat{H}'(t) = \hat{U}_0^\dagger(T,t)\hat{H}_0(T)\hat{U}_0(T,t)$.

The following subsections deal with different noise types according to their spectrum. We pay much attention to white noise because our method is perturbative, so understanding this reference case in depth is fundamental. In addition, white noise is amenable to analytical treatment and explicit optimization of trap trajectories.

1. White noise

The correlation function when $\xi(t)$ represents a white noise fluctuation is $\alpha(\tau) = \gamma\delta(\tau)$, and the corresponding power spectrum is constant, $S(\Omega) = \frac{\gamma}{2\pi}$. Here γ scales the noise and

$$g(t) = \gamma/2, f(t) = 0. \tag{26}$$

The instantaneous energy in Eq. (25) for an initial state in the $n_{\rm th}$ mode can be written as

$$\langle\hat{H}(T)\rangle = E(n) + \gamma G(T;n), \tag{27}$$

where

$$G(T;n) = \frac{m}{2}\int_0^T \ddot{x}_c^2(t)dt + \frac{\hbar\omega^3}{2}\left(n+\frac{1}{2}\right)T \tag{28}$$

is the "sensitivity" to noise. The excitation energy is $E_e = \gamma G(T;n)$. The first term of $G(T;n)$ contains an integral of $\ddot{x}_c(t)$ and the mass of the ion; it reflects the fact that larger displacements from the trap center [see Eq. (3)] increase the effect of spring constant fluctuations. The second term depends on the trap frequency and the final time, and it is independent of the trajectory, so it can only be reduced by speeding up the transport. For fixed T, however, it is possible to design the trajectory $x_c(t)$ to make $G(T;n)$ as small as possible and minimize the integral. We shall now consider four different protocols. Examples of the corresponding trap trajectories $x(t)$ are provided in Fig. 1(a).

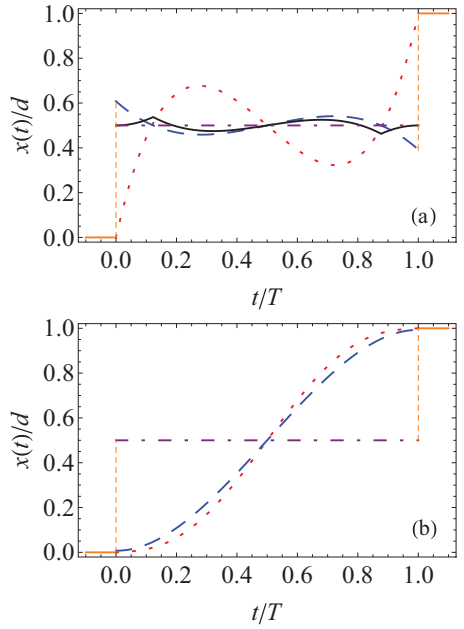

FIG. 1. (Color online) Comparison of trap trajectories x between the initial and final trap positions (yellow solid segments). Polynomial protocol (red dotted line); bounded optimal [black solid line, only in (a)]; unbounded optimal [blue dashed line, the jump at the boundary times is $6d/(\omega^2T^2)$]; bang-bang (dot-dashed purple line). In (a) $T = T_\omega/2$ (T_ω is the oscillation period); in (b) $T = 9T_\omega/2$. $\delta = 0.5\,d$, mass of $^{40}Ca^+$, initial state in $n = 0$, $\omega = 2\pi \times 1.4$ MHz, $d = 280\ \mu$m.

Polynomial protocol. A simple choice satisfying all boundary conditions and trap position continuity is a polynomial ansatz $x_c(t) = \sum_{n=0}^5 \beta_n t^n$. The β_n can be solved from the boundary conditions (7) and (8) to give

$$x_c(t) = d(10s^3 - 15s^4 + 6s^5), \tag{29}$$

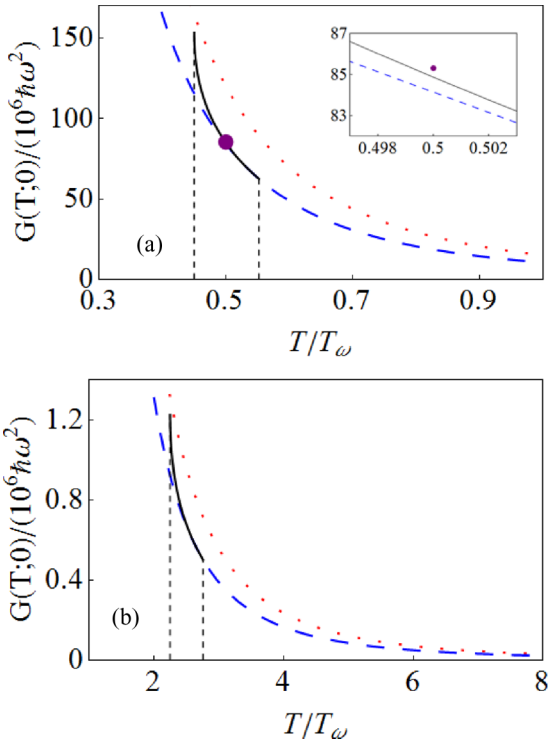

FIG. 2. (Color online) $G(T;0)$ versus final time. Polynomial ansatz (red dotted line), unbounded optimal (blue dashed line), bounded optimal [black solid line; the vertical dashed lines delimitate the time window in Eq. (34)], and bang-bang (purple dot, $T = T_\omega/2$; see the magnification in the inset). (a) $\delta = 0.5\,d$; (b) $\delta = 0.02\,d$; other parameters are the same as in Fig. 1.

where $s = t/T$, and the corresponding trap trajectory $x(t)$ is obtained from Eq. (3) (see Fig. 1). $G(T;n)$ becomes

$$G(T;n) = \frac{60md^2}{7T^3} + \frac{(2n+1)\hbar\omega^3}{4}T, \tag{30}$$

which is depicted in Fig. 2 (red dotted line) for $n = 0$. Short times are dominated by an inverse-cubic-in-time, frequency-independent term, and long times by a linear-in-time, d-independent term that accumulates the effect of noise. A minimum exists at $T = T_{\min} = \sqrt[4]{\frac{720md^2}{7(2n+1)\hbar\omega^3}}$. For the realistic parameters of the figures, $T_{\min} = 73.2\ T_\omega$, where $T_\omega = 2\pi/\omega$ is the oscillation period. This $T_{\min}$ is quite a large time (not shown in Fig. 2) well into the adiabatic regime.[1]

Optimal control. To minimize $G(T;n)$ for a given mode n and fixed transport time T, we may apply optimal control theory with the cost function,

$$J_E = \int_0^T \ddot{x}_c^2(t)dt = \int_0^T \omega^4 |x_c(t) - x(t)|^2 dt, \tag{31}$$

subjected to the conditions (7), and a constrained (bounded) displacement $|x_c(t) - x(t)| \leqslant \delta$. This optimal-control problem was worked out in [17] to minimize the time average of the potential energy. Incidentally, this also minimizes the small effects of fast ion shuttling on the internal states due to the dc Stark shift [29] and adverse effects arising from anharmonicities of the trap potentials [18]. The optimal $x_c(t)$ ($x(t)$ follows from Eq. (3) (see Fig. 1) [17]:

$$x_c(t) = \begin{cases} 0, & t \leqslant 0 \\ \frac{1}{2}\omega^2 t^2 \delta, & 0 < t < t_1 \\ -\frac{1}{6}\omega^2 a_1 (t - \frac{T}{2})^3 + v_0 t + a_2, & t_1 < t < t_1 + t_2 \\ d - \frac{1}{2}\omega^2 (t-T)^2 \delta, & t_1 + t_2 < t < T \\ d, & t \geqslant T \end{cases}, \tag{32}$$

where $a_1 = \frac{2\delta}{T - 2t_1}$, $v_0 = \frac{1}{4}\omega^2\delta(T + 2t_1)$, $a_2 = \frac{1}{2}(d - v_0 T)$, and $t_1 = \frac{T}{2}(1 - \sqrt{3}\sqrt{1 - \frac{4d}{\omega^2 T^2 \delta}})$. $G(T;n)$ becomes

$$G(T;n) = \hbar\omega^3 \left[\frac{m\omega}{2\hbar}\left(2\delta^2 t_1 + \frac{a_1^2 t_2^3}{12}\right) + \frac{2n+1}{4}T \right]. \tag{33}$$

These equations hold for the time window:

$$\sqrt{\frac{4d}{\omega^2\delta}} \leqslant T \leqslant \sqrt{\frac{6d}{\omega^2\delta}}. \tag{34}$$

For smaller times there is no solution to the "bounded control" optimization problem. For larger times, the solution coincides with the one for "unbounded control,"

$$x_c = d(3s^2 - 2s^3). \tag{35}$$

"Unbounded control" here means that the displacement is allowed to take any value, and this "unbounded" solution may be applied to an arbitrarily short time T [15,17,29]. The corresponding $G(T;n)$ is

$$G(T;n) = \frac{6md^2}{T^3} + \frac{(2n+1)\hbar\omega^3}{4}T, \tag{36}$$

similar in behavior to the polynomial ansatz [see Fig. 2 (blue dashed line)]. The minimum occurs at $T = \sqrt[4]{\frac{72md^2}{(2n+1)\hbar\omega^3}}$. For the parameters of the numerical examples, $T_{\min} = 66.9\ T_\omega$, again well into the adiabatic regime. The solid lines in Fig. 2 depict $G(T;n)$ in Eq. (33) for two values of the constraint.

Bang-bang protocol. Finally let us examine the simple bang-bang protocol [30]:

$$x(t) = \begin{cases} 0, & t \leqslant 0, \\ d/2, & 0 < t < T, \\ d, & t \geqslant T. \end{cases} \tag{37}$$

From Eq. (3), we can solve $x_c(t)$ as

$$x_c(t) = \frac{d}{2} - \frac{d}{2}\cos\omega t + \frac{d(1 + \cos\omega T)}{2\sin\omega T}\sin\omega t. \tag{38}$$

To make $x_c(t)$ satisfy the boundary conditions (7), the final time must be an odd multiple of a semiperiod, $\omega T = (2k+1)\pi$, $k = 0,1,2....$ Now,

$$G(T;n) = \frac{m\omega^4 d^2}{16}T + \frac{\hbar\omega^3(2n+1)}{4}T \tag{39}$$

increases linearly with time without a short-time inverse-cubic term characteristic of the previous protocols. For realistic parameters $m\omega d^2/(4\hbar) \gg 1$ so the increase of $G(T;n)$ with T is much faster than in the other protocols due to the

[1] A general bound for the time average of the potential energy $\overline{E_P}$ is [15] $\overline{E_P} \geqslant 6md^2/(T^4\omega^2)$. Thus $\overline{E_P} \approx \hbar\omega$, for the parameters of Fig. 1, requires transport times $T \geqslant 36\,T_\omega$.

first term in Eq. (39). For the minimal time, $T = T_\omega/2$, the $G(T;n)$ for a bang-bang approach is just slightly above that for the unbounded optimal protocol [see the inset in Fig. 2(a)]. Bang-bang $G(T;n)$ values for the next valid times ($3T_\omega/2$, $5T_\omega/2$...) are very high and out of scale in the figure. The unbounded optimal trajectory is quite close to the bang-bang one for $T = T_\omega/2$ but differs significantly from it for larger times [compare Figs. 1(a) and 1(b).

In specific quantum-information applications, the dependence of the noise sensitivity (28) with the shuttling time T and the noise intensity will play an important role to choose T and the transport protocol among the range of values attainable within the state-of-the-art technology. In particular, the minimal shuttling times accessible might be incompatible with high fidelity operations because of the increase of noise-induced excitation at short times in the optimal protocol. The usefulness of the bang-bang protocol is constrained, apart from the challenge to implement sharp jumps, by the fact that its minimal sensitivity occurs at half oscillation period. For such short shuttling times, all protocols, including the optimal, lead to relatively large noise sensitivities. However, optimal or smooth polynomial protocols decrease their sensitivity significantly for a range of larger times whereas the sensitivity for a bang-bang approach increases rapidly. In the perturbative regime considered here, these conclusions hold for colored noise as discussed in the next two subsections.

2. Ornstein-Uhlenbeck process

The Ornstein-Uhlenbeck (OU) noise is a natural generalization of the Markovian, white noise limit, with a finite correlation time τ and a power spectrum of Lorentzian form,

$$S(\Omega) = \frac{D}{2\pi(1+\Omega^2\tau^2)}, \tag{40}$$

where D is the noise intensity. It still provides analytical results. When $\tau \to 0$, it reduces to white noise, and is also instrumental in generating flicker noise (see the following subsection) by superposing a range of correlation times. The correlation function corresponding to Eq. (40) is

$$\alpha(t) = \frac{D}{2\tau}e^{-t/\tau}, \tag{41}$$

so that

$$g(t) = \frac{D}{2}(1-e^{-t/\tau}), \tag{42}$$

$$f(t) = \frac{D\tau}{2}\left(1-e^{-t/\tau}-\frac{t}{\tau}e^{-t/\tau}\right). \tag{43}$$

The energy in Eq. (25) will be

$$\langle \hat{H}(T)\rangle = E(n) + DG(T;n),$$

where the excitation energy is $E_e(T) = DG(T;n)$ and

$$G(T;n) = \frac{\hbar\omega^3}{4}(2n+1)(T-\tau+\tau e^{-T/\tau}) + \frac{m}{2}\int_0^T \left[(1-e^{-t/\tau})\ddot{x}_c^2(t) - \frac{\omega^2 t}{2\tau}e^{-t/\tau}\dot{x}_c^2(t)\right]dt.$$

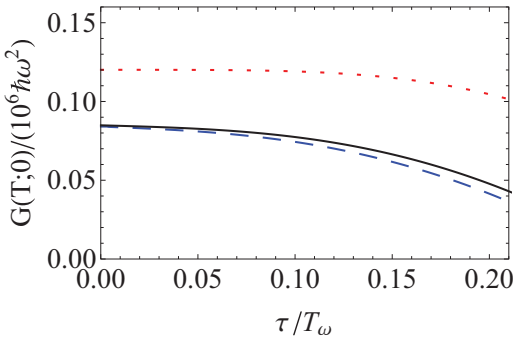

FIG. 3. (Color online) $G(T;0)$ for Ornstein-Uhlenbeck noise versus correlation time. Polynomial ansatz (red dotted line), unbounded optimal (blue dashed line), and bounded optimal (black solid line). $\delta = 0.005\,d$, $T = 5T_\omega$, and other parameters are the same as in Fig. 1.

In the small τ limit, integrating by parts and retaining only linear terms,

$$G(T;n) = \frac{\hbar\omega^3}{2}\left(n+\frac{1}{2}\right)(T-\tau) + \frac{m}{2}\left[\int_0^T \ddot{x}_c^2(t)dt - \tau\ddot{x}_c^2(0)\right]. \tag{44}$$

The two correcting terms proportional to τ are negative so that the noise effect is reduced with respect to white noise. In Fig. 3 we plot $G(T;0)$ versus correlation time using the polynomial protocol and the protocols (32) and (35) optimized for white noise.

3. Flicker noise

Flicker noise, with $\sim 1/\Omega$ spectrum in a range $\Omega_2 < \Omega < \Omega_1$, may be modeled by summing over Lorentzian (Ohrnstein-Uhlenbeck) noises [31,32] with proper statistical weights. Specifically we consider [31]

$$\alpha(t) = \frac{C}{\ln(\tau_2/\tau_1)}\int_{\tau_1}^{\tau_2}\frac{1}{\tau}e^{-t/\tau}d\tau, \tag{45}$$

where $C = \mathcal{E}[x^2(t)] = \alpha(0)$. Using Eq. (11), the corresponding power spectrum takes the form,

$$S(\Omega) = \frac{C}{\pi\ln(\tau_2/\tau_1)}\int_{\tau_1}^{\tau_2}\frac{d\tau}{1+\Omega^2\tau^2} = \begin{cases} \frac{(\tau_2-\tau_1)C}{\pi\ln(\tau_2/\tau_1)}, & \Omega \ll \Omega_2, \\ \frac{C}{2\ln(\tau_2/\tau_1)}\frac{1}{\Omega}, & \Omega_2 \ll \Omega \ll \Omega_1, \\ \frac{(\tau_2-\tau_1)C}{\pi\ln(\tau_2/\tau_1)}\frac{1}{\tau_1\tau_2\Omega^2}, & \Omega \gg \Omega_1, \end{cases} \tag{46}$$

where $\Omega_{1,2} = (2\pi)/\tau_{1,2}$. The spectrum is white if the frequency is below Ω_2 and decays as $1/\Omega^2$ above Ω_1. Equation (45) leads to

$$g(t) = \frac{C}{\ln(\tau_2/\tau_1)}\left[\tau - \tau e^{-t/\tau} - tEi\left(\frac{-t}{\tau}\right)\right]_{\tau_1}^{\tau_2}, \tag{47}$$

$$f(t)=\frac{C}{2\ln(\tau_2/\tau_1)}\times\left[\tau^2(1-e^{t/\tau})-t\tau e^{-t/\tau}-t^2 Ei\left(\frac{-t}{\tau}\right)\right]_{\tau_1}^{\tau_2}. \quad (48)$$

Here $Ei(-x)=\int_{-\infty}^{-x}(e^t/t)dt$ with $x>0$, which behaves as $Ei(-x)\simeq -e^{-x}/x$ for $x\to\infty$, and $Ei(-x)\simeq\gamma_E+\ln x$ for $x\to 0$, where γ_E is Euler's constant. The energy (25) takes the form,

$$\langle\hat{H}(T)\rangle=E(n)+\frac{2(\tau_2-\tau_1)C}{\ln(\tau_2/\tau_1)}G(T;n), \quad (49)$$

where the excitation energy is $E_e(T)=\frac{2(\tau_2-\tau_1)C}{\ln(\tau_2/\tau_1)}G(T;n)$ and

$$\begin{aligned}G(T;n)=&\frac{\hbar\omega^3}{4(\tau_2-\tau_1)}\left(n+\frac{1}{2}\right)\Big[\tau T(2-e^{-T/\tau})\\&+\tau^2(e^{-T/\tau}-1)-T^2 Ei\left(-\frac{T}{\tau}\right)\Big]_{\tau_1}^{\tau_2}\\&+\frac{m}{2(\tau_2-\tau_1)}\int_0^T\left\{\ddot{x}_c^2(t)\left[\tau-\tau e^{-t/\tau}-t\,Ei\left(-\frac{t}{\tau}\right)\right]_{\tau_1}^{\tau_2}\right.\\&\left.+\frac{\omega^2 t}{2}\dot{x}_c^2(t)Ei\left(-\frac{t}{\tau}\right)\Big|_{\tau_1}^{\tau_2}\right\}dt. \quad (50)\end{aligned}$$

For $\tau_2/T\ll 1$ and $\dot{x}_c(0)=0$, we find, integrating by parts, the approximation

$$\begin{aligned}G(T;n)\simeq&\frac{\hbar\omega^3}{2}\left(n+\frac{1}{2}\right)\left(T-\frac{\tau_2+\tau_1}{2}\right)\\&+\frac{m}{2}\left[\int_0^T\ddot{x}_c^2(t)dt-\frac{\tau_2+\tau_1}{2}\ddot{x}_c^2(0)\right], \quad (51)\end{aligned}$$

with a small correction to the white noise case similar to the one found for OU noise. Figure 4 depicts $G(T;0)$ versus τ_2 for the polynomial protocol and the protocols optimized in the Markovian limit.

For OU or flicker noise in the perturbative domain considered the conclusions found for white noise are largely applicable. The trap trajectory may be chosen to minimize the integral that appears in the sensitivity $G(T;0)$ regardless of the noise type. Apart from trap trajectories with sudden, finite position jumps (optimal trap trajectories unconstrained or constrained by a maximum ion displacement with respect to the center of the trap, and simple bang-bang trajectories), polynomial trajectories avoid the technical challenge of implementing sudden trap jumps. For very short shuttling times (half an oscillation period) optimal control and bang-bang solutions display a similar (relatively high) noise sensitivity. At moderate times and beyond (five oscillations or more) the bang-bang approach produces too much excitation and the polynomial behaves similarly to the optimal trajectory.

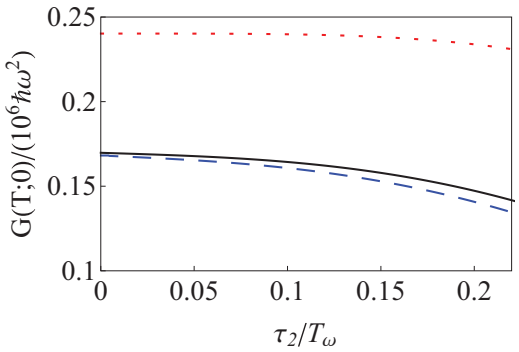

FIG. 4. (Color online) $G(T;0)$ for flicker noise versus upper limit of the interval of correlation times τ_2. Polynomial ansatz (red dotted line), unbounded optimal (blue dashed line), and bounded optimal (black solid line). $\delta=0.5\,d$, $\tau_1=1\times10^{-10}$ *s*, $T=5T_\omega$, and other parameters are the same as in Fig. 1.

B. Position noise

Suppose that the trap position fluctuates around the ideal trajectory $x(t)$ as $x(t)-K\xi(t)/(m\omega^2)$, where $\xi(t)$ is a random noise satisfying Eq. (10) and K is a constant. This corresponds to using $\hat{L}=(\hat{q}-x)K$ in Eqs. (9) and (13),

$$\hat{H}(t)=\frac{\hat{p}^2}{2m}+\frac{1}{2}m\omega^2[\hat{q}-x(t)]^2+\xi(t)K[\hat{q}-x(t)]. \quad (52)$$

The master equation (13) takes the form,

$$\begin{aligned}\frac{d}{dt}\hat{\rho}=&-\frac{i}{\hbar}[\hat{H}_0,\hat{\rho}]-\frac{K^2}{\hbar^2}g(t)[\hat{q}-x,[\hat{q}-x,\hat{\rho}]]\\&+\frac{K^2}{m\hbar^2}f(t)[\hat{q}-x,[\hat{p},\hat{\rho}]], \quad (53)\end{aligned}$$

where $g(t)$ and $f(t)$ have been defined in Eq. (15) and depend on the specific noise. Using the same time-dependent perturbation theory approach as in the previous section, the density operator is

$$\begin{aligned}\hat{\rho}(T)\simeq&\hat{\rho}_0(T)+\frac{K^2}{\hbar^2}\int_0^T g(t)\widetilde{U}_0(T,t)\widetilde{J}_2(t)\hat{\rho}_0(t)dt\\&+\frac{K^2}{m\hbar^2}\int_0^T f(t)\widetilde{U}_0(T,t)[\hat{q},[\hat{p},\hat{\rho}_0(t)]]dt,\end{aligned}$$

where the system energy is

$$\begin{aligned}\langle\hat{H}(T)\rangle=&\,\mathrm{tr}[\hat{H}_0(T)\hat{\rho}(T)]\simeq\langle\Phi(T;n)|\hat{H}_0(T)|\Phi(T;n)\rangle\\&+\frac{K^2}{\hbar^2}\int_0^T g(t)\langle\Phi(t;n)|\widetilde{J}_2(t)\hat{H}'(t)|\Phi(t;n)\rangle dt\\&+\frac{K^2}{m\hbar^2}\int_0^T f(t)\langle\Phi(t;n)|[\hat{p},[\hat{q},\hat{H}'(t)]]|\Phi(t;n)\rangle dt\\=&\,E(n)+\frac{K^2}{m}\int_0^T g(t)dt, \quad (54)\end{aligned}$$

when the ion starts in mode n. The excitation energy at the final time is independent of the trap trajectory and n, and depends only on the transport time and noise type. The only strategy left to minimize the effect of position fluctuations is to speed up the transport making T as small as possible. The independence on the trajectory may be understood already at a classical level from the solution of Eq. (3), $x_c(t)=x(t)-\int_0^t dt'\dot{x}(t')\cos[\omega(t-t')]$. Note that a deviation from $x_c(t)$ due to a modified trajectory $x(t)+\delta x(t)$ depends only on $\delta x(t)$ and its time derivative, not on $x(t)$ itself. As a consequence, studies of excitation or heating rates for nonshuttling traps are directly applicable [11,33–35].

Even in the case that position noise is dominant, the trajectories that minimize the effect of spring-constant noise are useful, since these trajectories minimize as well the time average of the potential energy [15,17], thus adverse effects of anharmonicity [18,36] are suppressed.

IV. SYSTEMATIC SPRING CONSTANT ERROR

Assume that the trap trajectory is designed for a given spring constant ω^2, but the actual one is different, $\omega^2(1+\Lambda)$. Λ may change from run to run but remain constant throughout the transport time. This is quite common as a consequence of experimental drifts and imperfect calibration. In current experiments it is likely to dominate other imperfections. Our objective here is to determine the induced excitation and to find trap trajectories that minimize the excitation in a range of Λ around 0. The system Hamiltonian is

$$\hat{H}(t) = \frac{\hat{p}^2}{2m} + \frac{1}{2}m\omega^2(1+\Lambda)[\hat{q} - x(t)]^2, \tag{55}$$

where Λ is the relative error in the spring constant. For the actual frequency, the auxiliary equation is

$$\ddot{x}_{c1}(t) + \omega_1^2(x_{c1} - x) = 0, \tag{56}$$

with $\omega_1^2 = \omega^2(1+\Lambda)$. We define $x_{c1}(t) = x_c(t) + F(t)$. Combining Eqs. (3) and (56), $F(t)$ satisfies

$$\ddot{F}(t) + \omega_1^2 F(t) = \Lambda \ddot{x}_c(t), \tag{57}$$

which is solved by

$$F(t) = \frac{\Lambda}{\omega_1}\sin(\omega_1 t)\int_0^t \ddot{x}_c(t')\cos(\omega_1 t')dt' - \frac{\Lambda}{\omega_1}\cos(\omega_1 t)\int_0^t \ddot{x}_c(t')\sin(\omega_1 t')dt'. \tag{58}$$

For the new frequency ω_1 and trajectory x_{c1}, the exact energy of the system takes the form,

$$\langle \hat{H}(T)\rangle = \left(n + \frac{1}{2}\right)\hbar\omega_1 + E_e(T), \tag{59}$$

where E_e is the excitation energy,

$$E_e(T) = \frac{m\Lambda^2}{2}\left[\int_0^T \ddot{x}_c(t)\cos(\omega_1 t)dt\right]^2 + \frac{m\Lambda^2}{2}\left[\int_0^T \ddot{x}_c(t)\sin(\omega_1 t)dt\right]^2. \tag{60}$$

To suppress the excitation energy, the trajectory $x_c(t)$ has to satisfy the conditions,

$$\int_0^T \ddot{x}_c(t)\cos(\omega_1 t)dt = 0, \quad \int_0^T \ddot{x}_c(t)\sin(\omega_1 t)dt = 0. \tag{61}$$

We approximate $\cos(\omega_1 t) \simeq \cos(\omega t)$ and $\sin(\omega_1 t) \simeq \sin(\omega t)$ to keep only quadratic terms in Λ in Eq. (60), and assume for x_c a seventh-order polynomial,

$$x_c(t) = \sum_{n=0}^{7} b_n t^n, \tag{62}$$

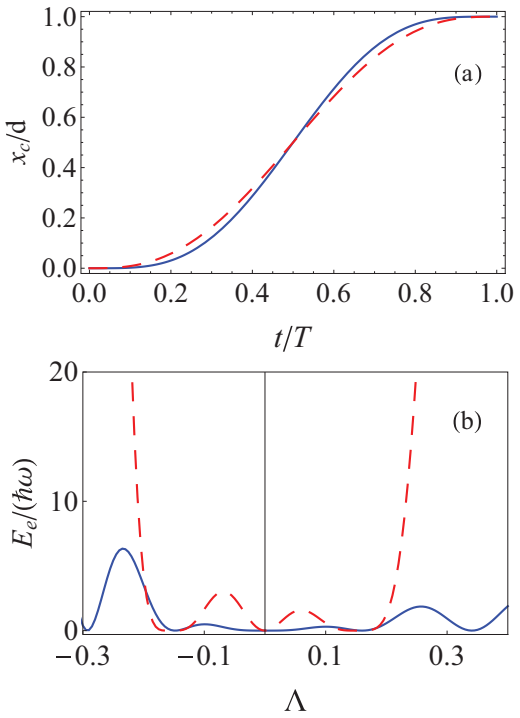

FIG. 5. (Color online) (a) $x_c(t)$ versus t; (b) excitation energy versus Λ. Dashed red line, quintic polynomial (29); solid blue line, seventh order polynomial in Eq. (62). $T = 6.5\,T_\omega$ and other parameters are the same as in Fig. 1.

to satisfy the six conditions in Eqs. (7) and (8) and

$$\int_0^T \ddot{x}_c(t)\cos(\omega t)\,dt = 0, \quad \int_0^T \ddot{x}_c(t)\sin(\omega t)\,dt = 0. \tag{63}$$

Doing the integrals formally, we end up with a system of eight equations with eight unknowns (the b_n), which can be solved, but the expressions for the b_n are too lengthy to be displayed here. The corresponding $x(t)$ is obtained from Eq. (3). In Fig. 5 we have plotted the seventh order x_c in Eq. (62) and the simplest quintic polynomial ansatz (29), as well as the corresponding excitation energies. The protocol based on Eq. (62) is more robust, i.e., it leads to smaller excitations when the actual trap frequency does not have the expected value. Alternative robustification schemes are possibly adapted to specific needs, for example, imposing zero or minimal excitation at a discrete number of values of Λ in a given interval (see, e.g., [37] for a similar approach applied to maximize the absorption of complex potentials).

Time-scaling errors are shown to be equivalent to spring-constant systematic errors in Appendix B, so the same strategies used here may be used in that case.

V. DISCUSSION

In this paper we have examined the excitation energy due to spring-constant noise or error and position noise in ions transported by a moving harmonic trap. We consider families of trajectories without final excitation in the noiseless limit and select optimal trap trajectories that minimize heating when the noise applies. For fixed shuttling time T, this selection is only

possible for spring-constant noise or error, since for position noise the final energy increases linearly with T but does not depend on any other feature of the trap trajectory.

Advances in the fabrication of microstructured ion traps and fast control electronics have allowed one to experimentally reach the limits of adiabacity, thus the proposed protocols may be tested and the respective noise sensitivity verified. Envisaged experiments at shuttle times of the order of an oscillation period [30] require changes of the trapping potential on time scales much shorter than the period corresponding to the trap frequency. At such fast temporal changes of the control voltages, the cutoff frequency for noise filtering elements must be very high, and thus we expect that it might be increasingly difficult to reach a low noise level. As additionally the noise sensitivity of the shuttling results is increasing at fast time scales, the importance of noise suppression by trajectory design becomes obvious. In the well-controlled setting of an ion trap, one may experimentally investigate the schemes with artificial injected designed noise [38,39]. It is within experimental reach to design the spectral properties of a noise source and verify the predicted effects. Besides the possibility of artificially injecting noise, the noise spectrum might depend on trap materials, electronic circuitry, and other elements amenable to being influenced by the experimentalist. The accuracy of sideband spectroscopy to determine the excess energy has reached a subphonon level, such that even small optimization effects would be visible.

ACKNOWLEDGMENTS

This work was supported by Grants No. 61176118, No. 12QH1400800, No. 13PJ1403000, No. 2013310811003, No. IT472-10, No. FIS2009-12773-C02-01, No. UFI 11/55, and the Program for Professor of Special Appointment (Eastern Scholar) at Shanghai Institutions of Higher Learning. This research was also funded by the Office of the Director of National Intelligence (ODNI), Intelligence Advanced Research Projects Activity (IARPA), through Army Research Office Grant No. W911NF-10-1-0284. The views and conclusions contained herein are those of the authors and should not be interpreted as representing the official policies or endorsements, either expressed or implied, of IARPA, the ODNI, or the US government.

APPENDIX A: CLOSED EQUATIONS FOR THE MOMENTS

The quadratic and linear operators involving position and momentum form a dynamical Lie algebra (the Hamiltonian is a member of this algebra) for the Hamiltonians that describe spring-constant noise and position noise. This leads to closed equations for the corresponding moments [35], which is interesting numerically, as the results are not perturbative in noise intensity. In addition, physical consequences follow without even solving the system as we shall see.

For spring constant noise, the expectation values of position and momentum operators and their quadratic combinations satisfy, using Eq. (20),

$$\frac{d}{dt}\begin{pmatrix}\langle\hat{q}^2\rangle\\ \langle\hat{p}^2\rangle\\ \langle\hat{q}\,\hat{p}+\hat{p}\hat{q}\rangle\\ \langle\hat{q}\rangle\\ \langle\hat{p}\rangle\end{pmatrix}=M_S\begin{pmatrix}\langle\hat{q}^2\rangle\\ \langle\hat{p}^2\rangle\\ \langle\hat{q}\,\hat{p}+\hat{p}\hat{q}\rangle\\ \langle\hat{q}\rangle\\ \langle\hat{p}\rangle\end{pmatrix}+\begin{pmatrix}0\\ 8\hbar^2x(t)^2g(t)\\ \frac{8\hbar^2}{m}x(t)^2f(t)\\ 0\\ m^2x(t)-\frac{4\hbar^2}{m}x(t)f(t)\end{pmatrix}, \tag{A1}$$

where

$$M_S=\begin{pmatrix}0 & 0 & \frac{1}{m} & 0 & 0\\ 8\hbar^2g(t) & 0 & -m\omega^2 & -16\hbar^2x(t)g(t) & 2m\omega^2x(t)\\ -2m\omega^2+\frac{16\hbar^2}{m}f(t) & \frac{2}{m} & 0 & 2m\omega^2x(t)-\frac{8\hbar^2}{m}x(t)f(t) & 0\\ 0 & 0 & 0 & 0 & \frac{1}{m}\\ 0 & 0 & 0 & -m\omega^2+\frac{4\hbar^2}{m}f(t) & 0\end{pmatrix}. \tag{A2}$$

For position noise, Eq. (53), the expectation values satisfy

$$\frac{d}{dt}\begin{pmatrix}\langle\hat{q}^2\rangle\\ \langle\hat{p}^2\rangle\\ \langle\hat{q}\,\hat{p}+\hat{p}\hat{q}\rangle\\ \langle\hat{q}\rangle\\ \langle\hat{p}\rangle\end{pmatrix}=M_P\begin{pmatrix}\langle\hat{q}^2\rangle\\ \langle\hat{p}^2\rangle\\ \langle\hat{q}\,\hat{p}+\hat{p}\hat{q}\rangle\\ \langle\hat{q}\rangle\\ \langle\hat{p}\rangle\end{pmatrix}+\begin{pmatrix}0\\ 2K^2g(t)\\ 2K^2f(t)/m\\ 0\\ m\omega^2x(t)\end{pmatrix}, \tag{A3}$$

where

$$M_P = \begin{pmatrix} 0 & 0 & 1/m & 0 & 0 \\ 0 & 0 & -m\omega^2 & 0 & 2m\omega^2 x(t) \\ -2m\omega^2 & 2/m & 0 & 2m\omega^2 x(t) & 0 \\ 0 & 0 & 0 & 0 & 1/m \\ 0 & 0 & 0 & -m\omega^2 & 0 \end{pmatrix}. \tag{A4}$$

For colored or white position noise, the average position and momenta are not affected by the noise.

APPENDIX B: TIME SCALING

We analyze here a systematic error in the clock used to design the trap trajectory so that instead of $x(t)$, the implemented trajectory is $x(\varepsilon t)$. The Hamiltonian is

$$\hat{H}(t) = \frac{\hat{p}^2}{2m} + \frac{1}{2}m\omega^2[\hat{q} - x(\varepsilon t)]^2, \tag{B1}$$

and the Schrödinger equation $i\hbar\partial\Psi(t)/\partial t = \hat{H}(t)\Psi(t)$ can be rewritten as

$$i\hbar\frac{\partial\chi(\tau)}{\partial\tau} = \hat{\mathcal{H}}(\tau)\chi(\tau), \tag{B2}$$

where $\tau = \epsilon t$, $\chi(\tau) = \Psi(t)$, and

$$\hat{\mathcal{H}}(\tau) = \frac{\hat{p}^2}{2m'} + \frac{1}{2}m'\omega'^2[\hat{q} - x(\tau)]^2, \tag{B3}$$

with $m' = \varepsilon m$, and $\omega' = \omega/\varepsilon$. Since $x(\tau)$ is designed for ω, time-scaling errors reduce formally to systematic spring-constant errors, and their effect can be suppressed or mitigated in the same manner.

[1] D. Kielpinski, C. Monroe, and D. Wineland, Nature (London) **417**, 709 (2002).
[2] M. A. Rowe, A. Ben-Kish, B. Demarco, D. Leibfried, V. Meyer, J. Beall, J. Britton, J. Hughes, W. M. Itano, B. Jelenković, C. Langer, T. Rosenband, and D. J. Wineland, Quant. Inf. Comput. **2**, 257 (2002).
[3] R. Reichle, D. Leibfried, R. B. Blakestad, J. Britton, J. D. Jost, E. Knill, C. Langer, R. Ozeri, S. Seidelin, and D. J. Wineland, Fortschr. Phys. **54**, 666 (2006).
[4] C. Roos, Physics **5**, 94 (2012).
[5] C. Monroe and J. Kim, Science **339**, 1164 (2013).
[6] J. P. Home, D. Hanneke, J. D. Jost, J. M. Amini, D. Leibfried, and D. J. Wineland, Science **325**, 1227 (2009).
[7] R. B. Blakestad, C. Ospelkaus, A. P. VanDevender, J. H. Wesenberg, M. J. Biercuk, D. Leibfried, and D. J. Wineland, Phys. Rev. A **84**, 032314 (2011).
[8] R. Bowler, J. Gaebler, Y. Lin, T. R. Tan, D. Hanneke, J. D. Jost, J. P. Home, D. Leibfried, and D. J. Wineland, Phys. Rev. Lett. **109**, 080502 (2012).
[9] A. Walther, F. Ziesel, T. Ruster, S. T. Dawkins, K. Ott, M. Hettrich, K. Singer, F. Schmidt-Kaler, and U. Poschinger, Phys. Rev. Lett. **109**, 080501 (2012).
[10] Q. A. Turchette, D. Kielpinski, B. E. King, D. Leibfried, D. M. Meekhof, C. J. Myatt, M. A. Rowe, C. A. Sackett, C. S. Wood, W. M. Itano, C. Monroe, and D. J. Wineland, Phys. Rev. A **61**, 063418 (2000).
[11] S. K. Lamoreaux, Phys. Rev. A **56**, 4970 (1997).
[12] M. Brownnutt *et al.* (unpublished).
[13] M. T. Baig, M. Johanning, A. Wiese, S. Heidbrink, M. Ziolkowski, and C. Wunderlich, Rev. Sci. Instr. **84**, 124701 (2013).
[14] R. Bowler, U. Warring, J. W. Britton, B. C. Sawyer, and J. Amini, Rev. Sci. Instr. **84**, 033108 (2013).
[15] E. Torrontegui, S. Ibanez, X. Chen, A. Ruschhaupt, D. Guéry-Odelin, and J. G. Muga, Phys. Rev. A **83**, 013415 (2011).
[16] E. Torrontegui, X. Chen, M. Modugno, S. Schmidt, A. Ruschhaupt, and J. G. Muga, New J. Phys. **14**, 013031 (2012).
[17] X. Chen, E. Torrontegui, D. Stefanatos, J.-S. Li, and J. G. Muga, Phys. Rev. A **84**, 043415 (2011).
[18] M. Palmero, E. Torrontegui, D. Guéry-Odelin, and J. G. Muga, Phys. Rev. A **88**, 053423 (2013).
[19] H. A. Fürst, M. H. Goerz, U. G. Poschinger, M. Murphy, S. Montangero, T. Calarco, F. Schmidt-Kaler, K. Singer, and C. P. Koch, arXiv:1312.4156.
[20] A. Ruschhaupt, X. Chen, D. Alonso, and J. G. Muga, New J. Phys. **14**, 093040 (2012).
[21] X.-J. Lu, X. Chen, A. Ruschhaupt, D. Alonso, S. Guérin, and J. G. Muga, Phys. Rev. A **88**, 033406 (2013).
[22] H. R. Lewis and W. B. Riesenfeld, J. Math. Phys. **10**, 1458 (1969).
[23] H. R. Lewis and P. G. Leach, J. Math. Phys. **23**, 2371 (1982).
[24] A. K. Dhara and S. V. Lawande, J. Phys. A **17**, 2423 (1984).
[25] L. Diósi, Quantum Semiclassic. Opt. **8**, 309 (1996).
[26] L. Diósi and W. T. Strunz, Phys. Lett. A **235**, 569 (1997).
[27] W. T. Strunz, Phys. Lett. A **224**, 25 (1996).
[28] T. Yu, L. Diosi, N. Gisin, and W. T. Strunz, Phys. Rev. A **60**, 91 (1999).
[29] Hoi-Kwan Lau and Daniel F. V. James, Phys. Rev. A **83**, 062330 (2011).
[30] J. Alonso, F. M. Leupold, B. C. Keitch, and J. P. Home, New J. Phys. **15**, 023001 (2013).
[31] F. N. Hooge and P. A. Bobbert, Phys. B **239**, 223 (1997).

[32] S. Watanabe, J. Korean Phys. Soc. **46**, 646 (2005).
[33] T. A. Savard, K. M. O'Hara, and J. E. Thomas, Phys. Rev. A **56**, R1095 (1997).
[34] M. E. Gehm, K. M. O'Hara, T. A. Savard, and J. E. Thomas, Phys. Rev. A **58**, 3914 (1998).
[35] S. Schneider and G. J. Milburn, Phys. Rev. A **59**, 3766 (1999).
[36] S. Schulz, U. Poschinger, K. Singer, and F. Schmidt-Kaler, Fortschr. Phys. **54**, 648 (2006).
[37] J. P. Palao, J. G. Muga, and R. Sala, Phys. Rev. Lett. **80**, 5469 (1998).
[38] Q. A. Turchette, C. J. Myatt, B. E. King, C. A. Sackett, D. Kielpinski, W. M. Itano, C. Monroe, and D. J. Wineland, Phys. Rev. A **62**, 053807 (2000).
[39] C. J. Myatt, B. E. King, Q. A. Turchette, C. A. Sackett, D. Kielpinski, W. M. Itano, C. Monroe, and D. J. Wineland, Nature (London) **403**, 269 (2000).